Spatial phase modulation due to the thermal nonlinearity in semiconductor-doped glasses

D. V. Petrov,* A. S. L. Gomes, and Cid B. de Araújo
Departamento de Física, Universidade Federal de Pernambuco, 50670-901 Recife, PE, Brazil
(Received 15 December 1993; revised manuscript received 12 May 1994)

We present experimental data and the underlying physics of spatial-phase-modulation effects associated with the thermal nonlinearity of semiconductor-doped glasses. Transient and steady-state self-focusing, laser-induced birefringence, and spatial ringing of the thermal origin were studied in this class of optical materials.

I. INTRODUCTION

Spatial phase modulation (SPM) of a laser beam has been extensively studied in the past years.[1-17] Among the several phenomena related to SPM are self-trapping and filamentation,[1,2] self- and cross-bending of light,[3,4] generation of spatial solitons,[5] and hexagonal pattern formation.[6]

Theoretically, these phenomena may be described by the wave equation which governs the propagation of a laser beam inside a nonlinear medium. The effect of the nonlinearity is included through an intensity-induced change in the sample's refractive index and intensity-dependent absorption. Models to study these phenomena have, for the most part, assumed a single-mode scalar electromagnetic field interacting with isotropic media and in general they have succeeded to give quantitative descriptions of various aspects of SPM. In principle, all kinds of media may exhibit SPM and a large amount of results has been reported for different materials. Among the nonlinear systems which exhibit large SPM, the semiconductor-doped glasses (SDG) represent an important class of optical materials for its potential applications in optical processing devices.

Studies related to SPM in the SDG have already been published which exploits the fast-electronic nonlinearity of this material.[9] On the other hand, the SDG thermal nonlinearity, which may be important under several experimental conditions,[10] has not been the object of more detailed studies.

It is the purpose of this paper to present a study of various aspects related to thermal SPM in SDG including effects of the laser field depolarization and temporal behavior. Although SDG have been extensively investigated in the past years, the kind of optical aberrations studied here was not reported before.

II. EXPERIMENTAL DETAILS

The experimental setup used is shown in Fig. 1. The excitation source was the second harmonic of a cw mode-locked Nd:YAG laser which delivers pulses of ~ 100 ps at 100 MHz. The laser beam intensity was monitored by the photodiode D_1 and the intensity at the sample position was adjusted using a half-wave-plate. The relative orientation of the two Glan prisms is adjusted in such a way that at low intensity no light is transmitted through the second Glan prism. An extinction ratio of 1000:1 was measured. Part of the beam with the same polarization as the incident laser was deflected by the Glan prism to the aperture and photodetector D_2.

The transmitted light through the Glan prism was analyzed using a camera coupled to a computer-controlled beam profile analyzer (Spiricon LBA 100). This system allowed us to study changes in the transverse profile of the transmitted beam which originates from the sample nonlinearity. The laser beam was focused using a 16-cm focal distance lens and the beam waist measured on the sample position was 43 μm.

In order to study the signal temporal behavior, an optical chopper was located before the beam splitter and the laser beam was modulated at 230 Hz with duty cycle of 50%. A boxcar integrator (gate = 15 μs) was used in connection with a computer to record the signal. The gate temporal position could be adjusted to study the signal at different times. For some experiments lock-in detection techniques have also been used.

A semiconductor-doped glass (Corning CS 3-68) was employed. This material is well known for its large electronic nonlinearity, $\chi^{(3)}$, and has been well characterized by several authors.[18,19] The Cd(S, Se) crystallite size in CS 3-68 glass is of ≈ 100 Å and their mutual distance is about 1000 Å, with a volume fraction of $< 1\%$. For the wavelength (532 nm) used in this work $\mathrm{Re}\chi^{(3)}$ is larger

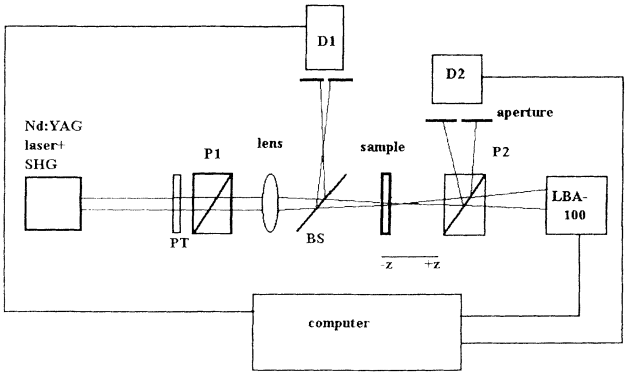

FIG. 1. Experimental arrangement used for the measurements.

than its imaginary part[18,19] but one-photon absorption is strong and causes a temperature increase in the focal region.

The transmission spectra of the sample (see Fig. 2) was measured using a grating spectrometer equipped with a tungsten lamp and the linear absorption coefficient at 532 nm is $\alpha_0=26\ \mathrm{cm}^{-1}$. The sample was mounted in a computer-controlled translation stage to allow direct measurements of the nonlinearity using the Z-scan technique.[17]

III. RESULTS AND DISCUSSIONS

As discussed by several authors[18] the SDG nonlinear response may be contributed by electron-hole pairs, trapping states, and thermal effects. In the present experiments, due to the laser frequency used and the high laser pulse repetition rate, the sample behavior is dominated by the thermal nonlinearity.

The temporal evolution of the transmitted signal, as measured by the photodetector D_2 with the aperture in the center of the laser spot, is illustrated in Fig. 3. The laser beam intensity was modulated as described in Sec. II. The z ordinate is measured along the beam direction and $z<0$ corresponds to locations of the sample between the lens and its focal plane (see Fig. 1). Note that the signal achieves its steady-state value in about 1.5 ms. Since the electronic relaxation occurs in a time interval $\leq 10\ \mu$s, we conclude that the observed temporal behavior is determined by the temperature distribution in the sample.

Of course, the time for establishment of the stationary temperature gradient, τ, depends not only on the material's properties but from the sample's geometric characteristics. In principle, the temperature effect can be modeled using transport equations involving the beam intensity, the temperature, and the electron-hole pair density.[10] However, our samples have transverse dimensions of 2–5 cm which are much larger than the laser beam waist and thus our results will not be affected by the shape of the samples. On the other hand, the carriers are confined to the Cd(S, Se) crystallites and do not diffuse.

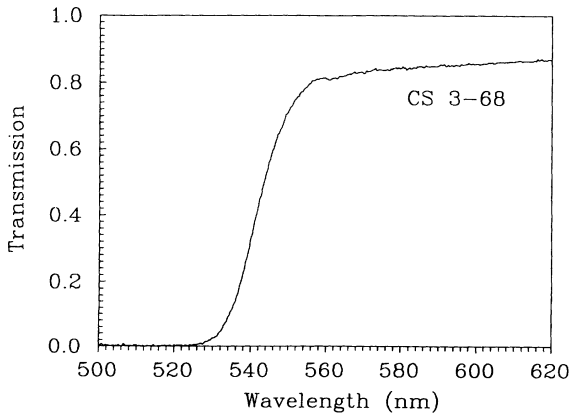

FIG. 2. Transmission spectra. Sample CS 3-68 (thickness: 0.21 cm).

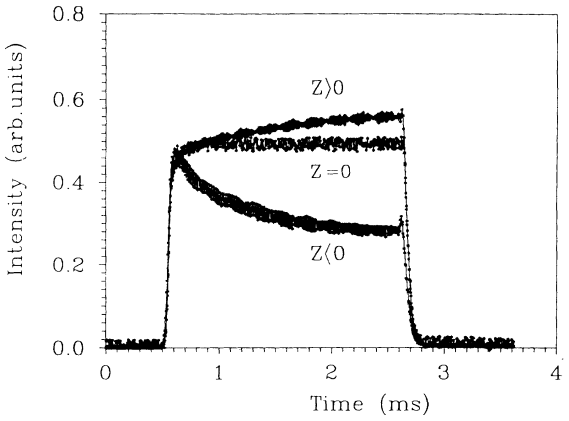

FIG. 3. Temporal behavior of the transmitted beam for different locations of the sample with respect to the focusing lens.

Therefore, we may use only the parameters of the borosilicate glass to estimate the thermal relaxation time,[20] which is given by $\tau=\rho c_p d_t^2/4K_1$, where ρ is the mass density, K_1 is the thermal conductivity, c_p is the specific heat at constant pressure, and d_t is the thermal diffusion length. Hence, assuming d_t equal to the spot size diameter (43 μm), $c_p=2.5\ \mathrm{J/cm^3\,°C}$ and $K_1=0.01\ \mathrm{W/cm\,°C}$,[10,20] we obtain $\tau\approx 1$ ms. This value is relatively close to the transient time shown in Fig. 3 and supports our interpretation for the observed temporal behavior as due to the thermal effects.

Therefore, the sample's nonlinear refractive index may be written as

$$n(r,t)=n_0+n_{2T}I\ , \tag{1}$$

with

$$n_{2T}=\frac{dn}{dT}f(\rho,c_p,\alpha,r,t)\ , \tag{2}$$

where n_0 is the linear refractive index, n_{2T} is the thermal nonlinear coefficient, and $f(\rho,c_p,\alpha,r,t)$ is a function which can be obtained from the transport equations mentioned above.

To determine n_{2T} we have used the simple and direct Z-scan technique,[17] which is based on the transformation of the laser wave front during beam propagation through a nonlinear sample, to amplitude distortion of the beam through an aperture in the far-field region. Information regarding the sign and magnitude of n_{2T} may be obtained by analyzing the transmitted beam intensity as a function of the sample distance from the focusing lens.

Signal detection was done using a boxcar with the gate located 1.8 ms after the chopped laser beam is switched on, in order to study the steady-state regime. The normalized transmittances for the sample studied are displayed in Figs. 4(a) and 4(b). The data were obtained moving the sample through the beam focal region using the computer-controlled stage. The peak-to-valley configuration of the Z-scan trace in Fig. 4(b) indicates a self-focusing nonlinearity ($n_{2T}>0$). The obtained values of the peak-to-valley transmission change, ΔT_{pv}, for mea-

surements with an open aperture ($S=1$) and small aperture ($S=0.025$) are so large that they cannot be described by the usual expressions for weak nonlinearities.[17] [Here, $S=1-\exp(-2r_a^2/W_a^2)$ is the aperture transmittance, r_a is the aperture radius, and W_a denotes the beam radius at the aperture for very low incident power (linear regime).]

Assuming that the effect of nonlinear absorption can be described as $\alpha(I)=\alpha_0+\beta I$ (where I is the irradiance of the laser beam inside the sample and β is the nonlinear absorption coefficient), we adjusted the experimental data to theory for $S=1$, using the exact expression for normalized energy transmittance:[17]

$$T(z)=\frac{1}{\sqrt{\pi}q_0(z)}\int_{-\infty}^{+\infty}\ln[1+q_0(z)e^{-t^2}]dt\ , \tag{3}$$

where $q_0(z)=\beta I_0 L_{\text{eff}}[(1+(z^2/z_0^2)]^{-1}$, I_0 is the on-axis intensity, $L_{\text{eff}}=(1-e^{-\alpha L})/\alpha$ is the effective sample length, L is the sample thickness, $z_0=k\omega_0^2/2$ is the diffraction length of the beam, ω_0 is the beam radius at $z=0$, and k is the wave number. The best fit was obtained for $\beta=5\times10^{-3}$ cm/W.

In principle, there are several contributions for the intensity-dependent absorption change such as population saturation, two-photon absorption, and thermal band-gap shift. The large values obtained for β can be explained by the reduction of the sample's band gap. It is possible to conclude from Fig. 2 that this red band-gap shift induces an increase in the absorption coefficient of the sample at 532 nm.

The expression for the on-axis normalized transmittance corresponding to small aperture ($S\sim0$) can be derived from Ref. (17) and is given by

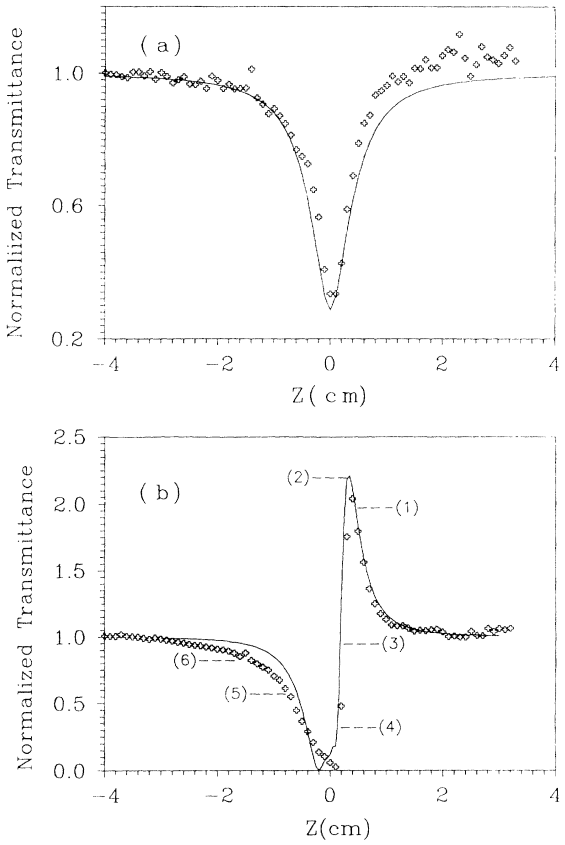

FIG. 4. (a) Normalized transmittance of the laser beam through the open aperture ($S=1$) vs the z position. Incident average power: 260 mW. (b) Normalized transmittance of the laser beam through the small aperture ($S=0.025$) vs the z position. Incident average power: 260 mW. The solid lines show the theoretical curves obtained as described in the text.

$$T(z)=\frac{\left|\sum_{m=0}^{\infty}\{[i\phi_0(z)]^m/m!\}\prod_{n=0}^{m}[1+i(2n-1)\beta/2kn_{2T}]\{g(z)+i[d/d_m(z)]\}^{-1}\right|^2}{\left|\{g(z)+i[d/d_0(z)]\}^{-1}\right|^2}\ , \tag{4}$$

where $\phi_0(z)=kn_{2T}I_0L_{\text{eff}}/[1+(z/z_0)^2]$, $g(z)=1+[d\cdot z/(z^2+z_0^2)]$, $d_m(z)=(k/2)[\omega_0^2/(2m+1)][1+(z/z_0)^2]$, and d is the propagation distance from the sample to the aperture plane. The best fit was obtained for $n_{2T}=4\times10^{-8}$ cm^2/W. This value is about three orders of magnitude larger than the electronic contribution to nonlinear effects.[18]

The most interesting results from our experiments were the spatial patterns observed through the Glan analyzer. In this case the large value of n_{2T} allows us to observe the beams's spatial pattern induced by the thermal nonlinearity.

In order to discuss our results let us consider first the material behavior observed when the analyzer axis is crossed with respect to the incident laser polarization. Figures 5(a) and 5(b) show the transverse intensity patterns corresponding to different positions of the sample along the beam direction. The numbers beside the patterns indicate the corresponding positions marked in Fig. 4(b). These transverse patterns look similar to the conventional patterns for a uniaxial calcite crystal cut perpendicular to the optical axis.[21] To explain the beam patterns we recall that in an isotropic medium, the nonzero components of the third-order susceptibility are $\chi^{(3)}_{1111}$, $\chi^{(3)}_{1122}$, $\chi^{(3)}_{1212}$, and $\chi^{(3)}_{1221}$ with $\chi^{(3)}_{1111}=\chi^{(3)}_{1122}+\chi^{(3)}_{1212}+\chi^{(3)}_{1221}$. It is known[2] that the induced nonlinear polarization has the same polarization state as the incoming beam, and therefore no change in the beam polarization is expected as a plane wave propagates in the medium. However, for a focused beam, polarization changes become possible. Indeed, let us consider two optical rays associated with the focused beam. Choose the coordinate axis z to be along the propagation direction and the x axis to be along the polarization of one of these rays. The

second ray propagates along a direction that has the angle $\theta \neq 0$ in the plane zy, whereas the angle between the x axis and the electric field of this ray is φ. The amplitude of the first ray is A, and the second ray has amplitude equal to B. These two rays will induce a nonlinear polarization with the y component given by $(\chi_{1212}+\chi_{1221})AB^2\cos\varphi\sin\theta\sin\varphi$. On the other hand, for each pair of rays associated with the focused incident beam with propagation directions corresponding to $\theta=0$ or at the xy plane ($\varphi=0$), there are no generated rays with orthogonal polarization. Hence, for any third-order nonlinear isotropic medium, the picture observed after the crossed polarizer should always have the dark cross in the middle. In our case the self-focusing effect, due to the thermal nonlinearity, is an additional and important source of light depolarization.

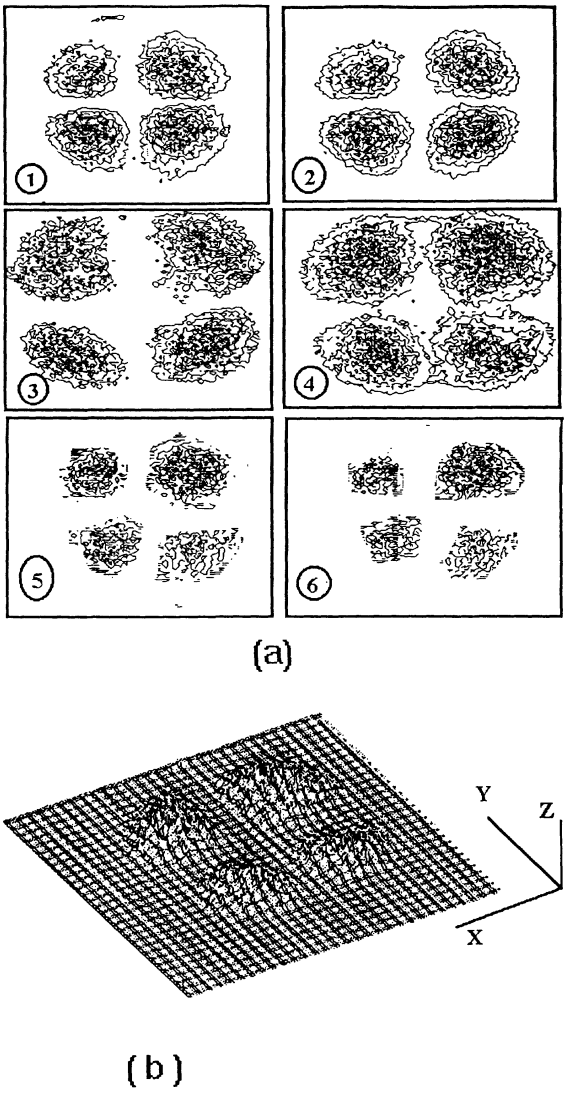

FIG. 5. (a) Transverse patterns measured through the Glan analyzer for six positions of the sample along the z axis. The numbers correspond to the positions indicated in Fig. 4(b). The density of lines is proportional to the light intensity. (b) Three dimensional intensity profile when the sample is located at position (4). The vertical axis is proportional to the light intensity and the (xy) plane is perpendicular to the beam propagation.

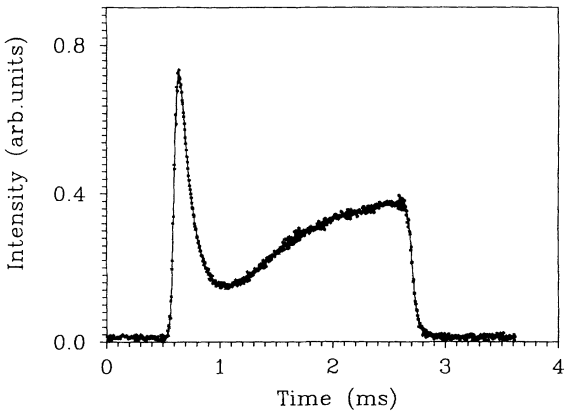

FIG. 6. Temporal behavior of the light intensity measured by a photodiode located at the region between the aberration ring and the central spot as discussed in the text.

When the analyzer axis is parallel to the incident laser polarization a spatial ring with circular symmetry surrounding the central spot is seen. A similar pattern has been originally observed in experiments with liquids[11] and recently this subject is receiving increasing atten-

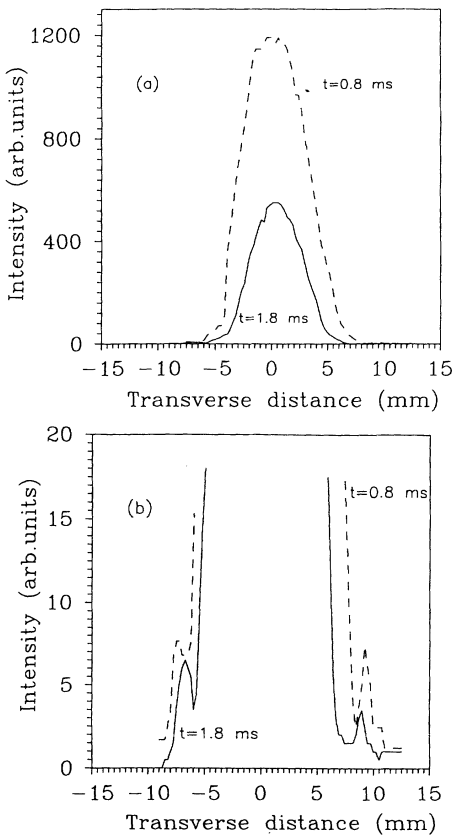

FIG. 7. (a) Transverse intensity profile obtained when the sample is placed at $z=0$ for two gate delays (solid line: 1.8 ms; dashed line: 0.8 ms). The electric-field polarization of the detected beam is parallel to the incident beam polarization. (b) Same profiles as in (a) with enlarged scale to show the temporal behavior of the aberration ring surrounding the central spot.

tion.[12–15] The ring structure may be explained as an interference effect between rays originating at the center of the beam and those far removed radially from the axis.[15,16] This effect is analogous in space of the self-induced spectral modulation instability,[2] i.e., spatial frequency sidebands are generated in the spatial beam profile. According to previous authors[12,15] the intensities of the rings, their diameter and their number depend strongly on the input intensity, the material's parameters, and the Fresnel numbers.

In our experiments only one interference ring was observed when the sample was located at $z=0$. However, we expect that a larger number of rings would be observed if larger laser intensities were available. On the other hand, the effect could not be observed in our experimental arrangement if an average power smaller than ~ 50 mW is focused on the sample.

Following the procedure of Refs. 13 and 14, we may estimate the refractive index change Δn in the beam center using the expression $\Delta n \cdot L_{\text{eff}} \simeq N\lambda$, where N is the number of rings. For the present case we have $L_{\text{eff}}=0.04$ cm and $\Delta n = 0.9\times 10^{-3}$. This change in the refractive index has the same order of magnitude as obtained in the Z-scan experiments.

In another experiment we have studied the buildup of the self-focusing process leading to the optical aberrations discussed above. First we have observed that the temporal behavior of the signal from photodiode D_2 was dependent on the position across the beam transverse direction. In particular we show in Fig. 6 the oscilloscope trace observed when the photodiode was placed somewhere between the ring and the main lobe. The oscilloscope trace indicates that before the steady-state regime there is an important change in the transverse energy distribution. This indication was corroborated by two other measurements using the boxcar and locating its gate at 0.8 and 1.8 ms after the beginning of the light pulse. The results shown in Fig. 7 indicate a shift of the ring towards the spot center. This effect may be explained in the following way. First we recall that Δn is dependent on the sample temperature. Since a sufficient amount of energy is carried by the light beam, a rapid increase of Δn takes place at the beginning of the light pulse and before transverse heat diffusion becomes important. Later, when the steady-state regime is approached, Δn assumes smaller values and the ring diameter is continuously reduced. For a gate delay of 1.8 ms the steady-state regime was already established and the corresponding transverse profile indicates the final-energy distribution of the transmitted beam corresponding to the Δn value indicated above.[22]

IV. SUMMARY

In summary, we have demonstrated a number of spatial-phase-modulation phenomena for semiconductor-doped glasses. The observed far-field transverse patterns depend on the laser frequency, input beam intensity, and symmetry of the experiment. The relevant dynamical behavior of the studied effects occurs in the ms range and is essentially governed by the thermal nonlinearity of the samples.

ACKNOWLEDGMENTS

We thank Lucio H. Acioli for stimulating discussions at the initial stage of this work and Renato E. de Araújo for his help with the data acquisition system during the whole experiment. This work was partially supported by the Brazilian Agencies Conselho Nacional de Desenvolvimento Científico e Tecnológico (CNPq) and Financiadora Nacional de Estudos e Projetos (FINEP). One of us (D.V.P.) also thanks the International Science Foundation for partial support.

*Permanent address: Institute of Semiconductor Physics (Novosibirsk, Russia).

[1]For a review of earlier studies, see Y. R. Shen, Prog. Quant. Electron. **4**, 1 (1975); J. H. Marburger, *ibid.* **4**, 35 (1975).

[2]Y. R. Shen, *The Principles of Nonlinear Optics* (Wiley, New York, 1984).

[3]A. E. Kaplan, Pis'ma Zh. Eksp. Teor. Fiz. **9**, 58 (1969) [JETP Lett. **9**, 33 (1969)]; G. A. Swartzlander and A. E. Kaplan, J. Opt. Soc. Am. B **5**, 765 (1988); Q. Xing, K. M. Yoo, and R. R. Alfano, Opt. Lett. **18**, 479 (1993).

[4]I. Golub, Opt. Commun. **89**, 289 (1992); Y. Li, D. Y. Chen, L. Yang, and R. R. Alfano, Opt. Lett. **16**, 4438 (1991).

[5]S. Maneuf, R. Degailly, and C. Froehly, Opt. Commun. **65**, 193 (1988); J. S. Aitchison, A. M. Weiner, Y. Silberberg, M. K. Oliver, J. L. Kackel, D. E. Leaird, E. M. Vogel, and D. W. Smith, Opt. Lett. **15**, 471 (1990).

[6]G. Grynberg, E. Le Bihan, P. Verkerk, P. Simoneau, J. R. Rios Leite, D. Bloch, S. LeBoiteux, and M. Ducloy, Opt. Commun. **66**, 321 (1988); W. J. Firth, A. J. Scroggie, G. S. McDonald, and L. A. Lugiato, Phys. Rev. A **46**, R3609 (1992); T. Honda, Opt. Lett. **18**, 598 (1993).

[7]G. P. Agrawal, Phys. Rev. Lett. **64**, 2487 (1990); J. Opt. Soc. Am. B **7**, 1072 (1990); C. J. McKinstrie and G. G. Luther, Phys. Scr. **30**, 31 (1990); R. Chang, W. J. Firth, R. Indik, J. V. Moloney, and E. M. Wright, Opt. Commun. **88**, 167 (1992).

[8]See, for example, N. B. Abraham and W. J. Firth, J. Opt. Soc. Am. B **7**, 951 (1990), and references therein.

[9]J. M. Hickmann, A. S. L. Gomes, and Cid B. de Araújo, Phys. Rev. Lett. **68**, 3547 (1992); H. Ma, A. S. L. Gomes, and Cid B. de Araújo, Appl. Phys. Lett. **59**, 2666 (1991); J. Opt. Soc. Am. B **9**, 2230 (1992); Opt. Commun. **87**, 19 (1992); H. Ma and Cid B. de Araújo, Appl. Phys. Lett. **63**, 3553 (1993).

[10]G. Thibault and M. M. Denariez-Roberge, Can. J. Phys. **63**, 198 (1985); M. Bertolotti, G. Liakhou, F. Michelotti, F. Senesi, and C. Sibilia, Pure Appl. Opt. **1**, 145 (1992).

[11]S. A. Akhmanov, D. P. Krindack, A. P. Sukhorukov, and R. V. Khokhov, Pis'ma Zh. Eksp. Teor. Fiz. **6**, 509 (1967) [JETP Lett. **6**, 38 (1967)].

[12]W. Du and S. Liu, Opt. Commun. **98**, 117 (1993); H. J. Zhang, J. H. Dai, P. Y. Wang, and L. A. Wu, Opt. Lett. **14**, 695 (1989); I. C. Khoo, J. Y. Hou, T. H. Liu, P. Y. Yan, R. R. Michel, and G. M. Finn, J. Opt. Soc. Am. B **4**, 886 (1987).

[13]S. D. Durbin, S. M. Arakelian, and Y. R. Shen, Opt. Lett. **6**, 411 (1981).

[14]M. Horowitz, R. Daisy, O. Werner, and B. Fischer, Opt. Lett **17**, 475 (1992).

[15]M. Le Berre, E. Ressayre, A. Tallet, K. Tai, H. M. Gibbs, M. C. Rushford, and N. Peyghambarian, J. Opt. Soc. Am. B **1**, 591 (1984); M. Le Berre, E. Ressayre, and A. Tallet, Phys. Rev. A **25**, 1604 (1982).

[16]F. W. Dabby, T. K. Gustafson, J. R. Whinnery, Y. Kohanzadeh, and P. L. Kelly, Appl. Phys. Lett. **16**, 362 (1970).

[17]M. Sheik-Bahae, A. A. Said, T. H. Wei, D. J. Hagan, and E. M. Van Stryland, IEEE J. Quantum Electron. **QE-26**, 760 (1990).

[18]For a review and further references, see C. Flytzanis, F. Hache, M. C. Klein, D. Ricard, and P. Roussignol, in *Progress in Optics,* edited by E. Wolf (North-Holland, Amsterdam, 1991), Vol. XXIX, p. 321

[19]P. Roussignol, D. Ricard, and C. Flytzanis, Appl. Phys. A **44**, 285 (1987); V. S. Williams, G. R. Olbright, B. D. Flugel, S. W. Koch, and N. Peyghambarian, J. Mod. Opt. **35**, 1979 (1988); H. Ma, A. S. L. Gomes, and Cid B. de Araújo, Opt. Lett. **16**, 630 (1991).

[20]J. R. Gordon, R. C. C. Leite, R. S. Moore, S. P. S. Porto, and J. R. Whinnery, J. Appl. Phys. **36**, 3 (1965); M. Bertolotti, A. Ferrari, C. Sibilia, G. Suber, D. Apostol, and P. Jani, Appl. Opt. **27**, 1811 (1988).

[21]M. Born and E. Wolf, *Principles of Optics,* 6th ed. (Pergamon, Oxford, 1980).

[22]All effects reported here were also observed by us using other types of SDG, absorbing at 532 nm, as well as for glass filters without semiconductor crystallites but with a comparable linear absorption coefficient. These results give further evidence for the dominant role of the thermal nonlinearity in our experiments.

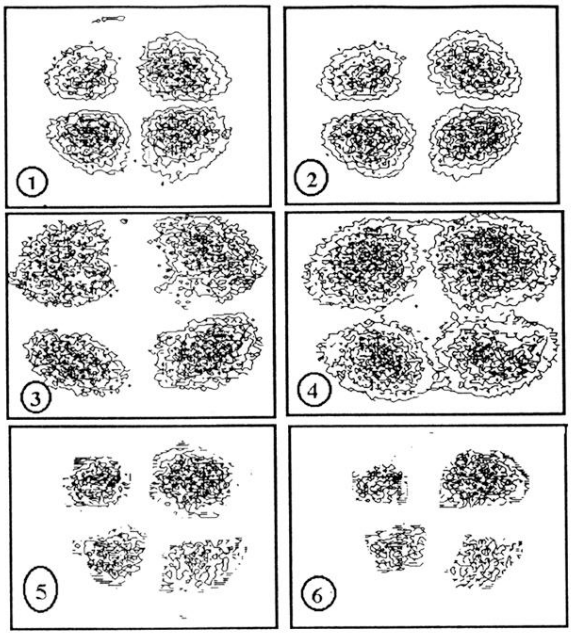

(a)

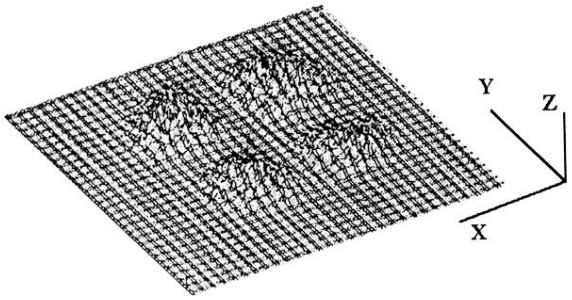

(b)

FIG. 5. (a) Transverse patterns measured through the Glan analyzer for six positions of the sample along the z axis. The numbers correspond to the positions indicated in Fig. 4(b). The density of lines is proportional to the light intensity. (b) Three dimensional intensity profile when the sample is located at position (4). The vertical axis is proportional to the light intensity and the (xy) plane is perpendicular to the beam propagation.